ACS OMEGA

http://pubs.acs.org/journal/acsodf

Article

Characteristics of a Novel Decomposed Corn Straw-Sludge Biochar and Its Mechanism of Removing Cadmium from Water

Qiaoting Chen, Minling Gao,* Qiyu Miao, Ling Xiao, Zhongyang Li, Weiwen Qiu, and Zhengguo Song*

Cite This: *ACS Omega* 2023, 8, 24912−24921

Read Online

ACCESS | Metrics & More | Article Recommendations | Supporting Information

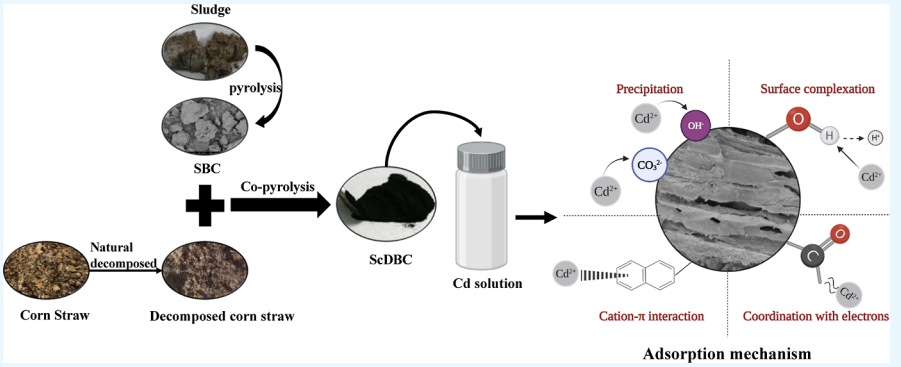

ABSTRACT: The utilization of high-efficiency adsorption materials to reduce cadmium pollution in aquatic environments is the focus of current environmental remediation research. Straw waste and sludge, which are available in huge amounts, can be best utilized in the preparation of environmental remediation materials. In this study, six types of biochar (SBC, CBC, DBC, SD_1BC, S_RDBC, and S_CDBC) were prepared from straw and sludge by co-pyrolysis, and their cadmium adsorption mechanisms were explored. Cd(II) adsorption isotherms and kinetics on the biochar were determined and fitted to different models. Kinetic modeling was used to characterize the Cd(II) adsorption of biochar, and findings revealed the process of sorption followed pseudo-second-order kinetics ($R^2 > 0.96$). The Langmuir model accurately represented the isotherms of adsorption, indicating that the process was monolayer and controlled by chemical adsorption. S_CDBC had the highest capacity for Cd(II) adsorption (72.2 mg g^{-1}), 1.5 times greater than that of sludge biochar, and 3 times greater than that of corn straw biochar. As the pH level rose within the range of pH 5.0 to 7.0 and the ionic strength decreased, the adsorption capacity experienced an increase. S_CDBC contained $CaCO_3$ mineral crystals before Cd(II) adsorption, and $CdCO_3$ was found in S_CDBC after adsorbing Cd(II) via X-ray diffraction analysis; the peak of Cd could be observed by Fourier transform infrared spectroscopy after the adsorption of Cd(II). The possible adsorption of Cd(II) by S_CDBC occurred primarily via surface complexation with active sorption sites, precipitation with inorganic anions, and coordination with π electrons. Collectively, the study suggested that the six types of biochar, particularly S_CDBC, could be used as highly efficient adsorbents for Cd(II) removal from aquatic environments.

1. INTRODUCTION

Water pollution caused by heavy metals is a challenging problem that posed a threat to ecosystems, the environment, and human health worldwide.[1] The most commonly used heavy metal removal methods contained adsorption, photocatalysis, chemical precipitation, ion exchange, electrochemical approaches, membrane filtering, and forward osmosis.[2,3] Cadmium (Cd) poisoning can lead to lung damage, cancer, hypertension, liver disease, and aberrant physiological development. Owing to its high persistence, solubility, mobility, and bioaccumulation, Cd is listed as China's priority pollutant and as one of the most contaminating heavy metals;[4,5] therefore, removal of Cd from the aquatic environment is highly important. Ion exchange, chemical precipitation, coagulation, adsorption, and membrane separation are common methods used to remove Cd(II) from aquatic environment. Among them, biochar adsorption has broad application prospects in wastewater remediation.[6]

Biochar is an incompletely carbonized organic substance with a complex surface chemical structure, more micropore structure, and excellent adsorption performance.[7] It is usually prepared by pyrolyzing biomass, such as plant straw, animal manure, and sewage sludge, at high temperatures in oxygen-limiting circumstances.[8] Cd(II) removal by biochar had been

Received: February 28, 2023
Accepted: June 14, 2023
Published: June 30, 2023

reported earlier; Higashikawa et al.[9] reported that Cd(II) removal impact and sorption mechanism of biochar are affected by various factors, including the type of raw material, pyrolysis temperature, and adsorption conditions.

Sludge is composed of organic compounds, macro- and micronutrients, trace elements, microorganisms, and micro pollutants.[10] After pyrolysis and carbonization, biochar can be used as a cheap raw material for the preparation of biochar adsorbents.[11,12] With the continued development of urbanization, the vast volume of urban sludge has become a severe ecological burden. Treatment methods, such as aerobic or anaerobic digestion, incineration, composting, landfill, and direct agricultural utilization, not only consume energy but may also cause additional environmental risks.[13] China is a big agricultural country with rich straw resources. The annual output of straw exceeds 1.0×10^{10} tons (40% of that of corn straw), accounting for more than 15% of the total output of agricultural straw.[14,15] The utilization rate of corn straw is low, and more than half of it is burnt, causing air pollution.[16]

Under these circumstances, sludge and corn straw were found to be quite suitable for the production of biochar to achieve resource utilization. Several studies on biochar preparation by co-pyrolysis of straw and sludge have shown that co-pyrolysis cannot only compensate for the defects of sludge with large ash content, less volatile substances, and low carbon content but also lessen the heavy metal risks of biochar by diluting the sludge's heavy metal concentration.[17−19] Wang et al.[20] reported that biochar produced by co-pyrolysis of sludge and wheat straw has a higher porosity and a larger specific surface area than pure sludge biochar.

However, relatively few investigations have been conducted to date on the influence of sludge on the performance of decomposed straw biochar. According to Zhang et al.,[21] carboxylic acid esters are decomposed, carboxyl groups are increased, and organic acids are formed during the decomposition of corn straw. Changes on the straw surface in functional groups may result in the formation of humus, thus improving the adsorption performance of biochar. Wang et al.[20] reported that sludge-corn straw biochar exhibits high Cr(VI) sorption capacity. We hypothesized that the increased biomass would improve the adsorption of heavy metals by biochar prepared by adding sludge to a co-pyrolysis mix of decomposed straw.

Biochar made from decomposed straw and sludge has not yet been implemented to remove Cd(II) from the aquatic environment. Therefore, in this study, sludge and decomposed corn straw were utilized as raw materials to prepare biochar. This study aimed to demonstrate the facile fabrication of biochar utilizing decomposed straws and sludge. Furthermore, the sorption characteristics of six different types of biochar were investigated, including sorption kinetics and isotherm adsorption, as well as the impact of pH and ionic strength on Cd(II) adsorption. Additionally, this study delved into understanding the sorption mechanism involved.

2. MATERIALS AND METHODS

2.1. Reagents and Materials. Sodium hydroxide (NaOH), cadmium nitrate [$Cd(NO_3)_2{\cdot}4H_2O$], and nitric acid (HNO_3) were provided by Jiuxinyaozheng Co. Ltd., (Beijing, China). All chemicals used in the investigations were of analytical quality, and all experiments were conducted with deionized water (18.25 MΩ cm^{-1}).

Corn straw was obtained from farmland in Tianjin, China. Sewage sludge was obtained from an urban domestic sewage treatment plant in Shantou, China. The inductively coupled plasma mass spectrometry test results for municipal sludge have been reported in the Supporting Information.

2.2. Preparation of Biochars. Sludge from the sewage treatment plant was used as a raw material, which was dried and put through a 0.25 mm sieve to obtain sludge powder in the laboratory. Before usage, corn straw was dried at 80 °C in the oven, pulverized, and passed through a 0.25 mm sieve. The six methods of preparation of biochar were as follows: (1) SBC: sludge was dried to a consistent weight before being pulverized, sieved, and pyrolyzed into sludge biochar. (2) CBC: corn straw was dried to a consistent weight before being pulverized, sieved, and pyrolyzed into straw biochar. (3) DBC: corn straw was placed in white plastic buckets, an appropriate amount of water was added, and it was placed under natural conditions for 30 d to let it mature to black naturally. After decomposition, the sample was dried to a consistent weight before being pulverized, sieved, and pyrolyzed into biochar. (4) SD_1BC: the sludge: corn straw mass ratio of 1:3 was physically mixed, and a suitable amount of water was supplied; it was placed in plastic buckets with intermittent oxygen supply in the early stage and placed under natural conditions for 30 d to allow it to mature naturally. (5) S_RDBC: a mass ratio of sludge: decomposed straw = 1:3 was physically mixed and pyrolyzed into biochar. (6) S_CDBC: a mass ratio of sludge biochar: decomposed straw = 1:3 was physically mixed and pyrolyzed thereafter.

Pyrolysis was used to prepare biochar,[22] and the process was conducted in a muffle furnace with a nitrogen flow rate of 6000 cm^3 min^{-1} and a temperature ranging from ambient to 600 °C for a duration of 1 h. The biochar was prepared, washed with deionized water, and then dried for 24 h at 60 °C in the oven.

2.3. Cd (II) Sorption. Six biochar samples (0.5 g) were added to a 250 mL solution containing 100 mg L^{-1} of Cd(II) to perform the kinetics experiment and then stored in 0.5 mL aliquots at pH 6.0 at intervals of 1, 5, 10, 20, 30, 60, 120, 240, 360, 480, 720, 1440, and 2160 min. Furthermore, the rotor was set to turn at 350 rpm, and the temperature was set to 25 ± 1 °C. The sample was filtered through a 0.22 μm filter and analyzed using atomic absorption spectrometry (AAS) (Beijing Haiguang). Adsorption performance in Cd(II) solution was compared in terms of concentration decrease.

The adsorption quantity (qt) was estimated according to the following equation

$$q_t = \frac{(c_0 - c_t)V}{m} \tag{1}$$

where qt represents the Cd(II) adsorbed quantity at time t (mg g^{-1}), m represents the weight of biochar used (g), c_0 represents the initial concentration (mol L^{-1}), and c_t represents the time concentration (mol L^{-1}).

OriginPro was used to fit q_t and t to the pseudo-first-order and pseudo-second-order kinetic models.

The equation below describes the pseudo-first-order kinetic model

$$q_t = q_e{}^*(1 - e^{-k_1 t}) \tag{2}$$

where q_t represents the Cd(II) adsorbed quantity at time t (mg g^{-1}), q_e represents the equilibrium adsorption quantity, t

https://doi.org/10.1021/acsomega.3c01196
ACS Omega 2023, 8, 24912−24921

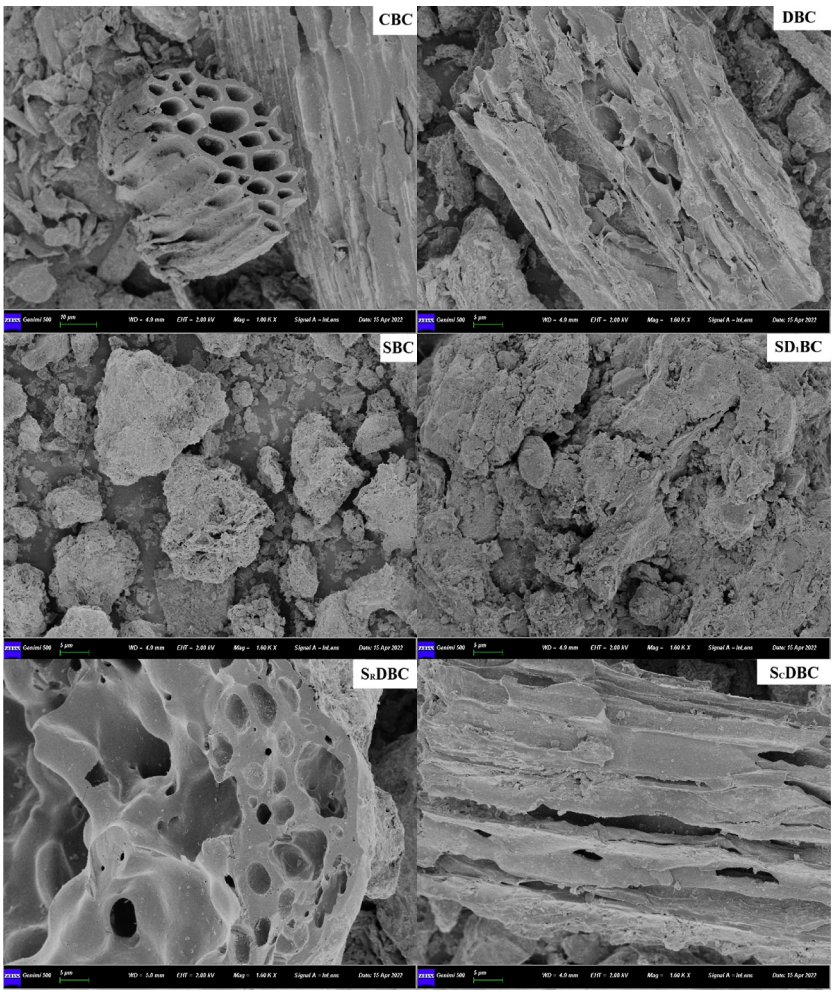

Figure 1. SEM images of different biochars before adsorption of Cd(II).

represents the adsorption duration, and k_1 represents the pseudo-first-order rate constant (min^{-1}).

The equation below describes the pseudo-second-order kinetic model

$$q_t = \frac{q_e^{\,2} \times k_2 \times t}{1 + q_e \times k_2 \times t} \tag{3}$$

where q_t represents the Cd(II) adsorbed quantity at time t (mg g^{-1}), t represents the adsorption duration, q_e represents the equilibrium adsorption quantity, and k_2 represents the pseudo-secondary rate constant [g $(mg{\cdot}min)^{-1}$].

All equilibrium adsorption isotherms were obtained with 0.01 g of adsorbent and 20 mL of Cd(II) solution [concentrations of 10, 25, 50, 80, 100, 150, and 200 mg L^{-1} (pH 6.0)] in 40 mL brown glass bottles. NaOH or HNO_3 solution (0.1 mol L^{-1}) was used to modify the solution's pH. By adjusting the solution's pH to 5.0−7.0, the impact of pH on the Cd(II) adsorption was evaluated. $NaNO_3$ (0.001−0.1 mol L^{-1}) was used to examine the ionic strength. Finally, the adsorption equilibrium was obtained by end-oscillating in a thermostatic oscillator for 36 h at 25 ± 0.5 °C and 120 rpm. Whatman no. 42 filter paper was then used to filter the suspension. Furthermore, AAS was used to determine the equilibrium concentration of Cd (II) in the filtrate. Triplicates of all batch adsorption experiments were performed. Based on the decrease in Cd(II) of the solution, the performance of Cd(II) adsorption was compared.

The adsorbed amount (q_t) was calculated according to

$$q_e = \frac{(c_0 - c_e)V}{m} \tag{4}$$

where q_e represents the adsorbed Cd(II) quantity (mg g^{-1}), c_0 represents the initial concentration (mol L^{-1}), c_e represents the equilibrium concentration (mol L^{-1}), and m represents the amount of biochar used (g).

The equation below describes the Langmuir model

$$q_e = \frac{k_4 \times c_e \times q_m}{1 + k_4 \times c_e} \tag{5}$$

where q_e represents the adsorbed balance Cd(II) quantity (mg g^{-1}), c_e represents equilibrium concentration (mol L^{-1}), k_4 represents the Langmuir constant, and q_m represents the maximum quantity of adsorbed Cd(II) (mg g^{-1}).

The equation below describes the Freundlich model

$$q_e = k_5 \times c_e^{\,1/n} \tag{6}$$

where q_e represents the balance quantity of adsorbed Cd(II) (mg g^{-1}), c_e represents the equilibrium concentration (mol L^{-1}), and k_5 and n represent the Freundlich constants.

https://doi.org/10.1021/acsomega.3c01196
ACS Omega 2023, 8, 24912−24921

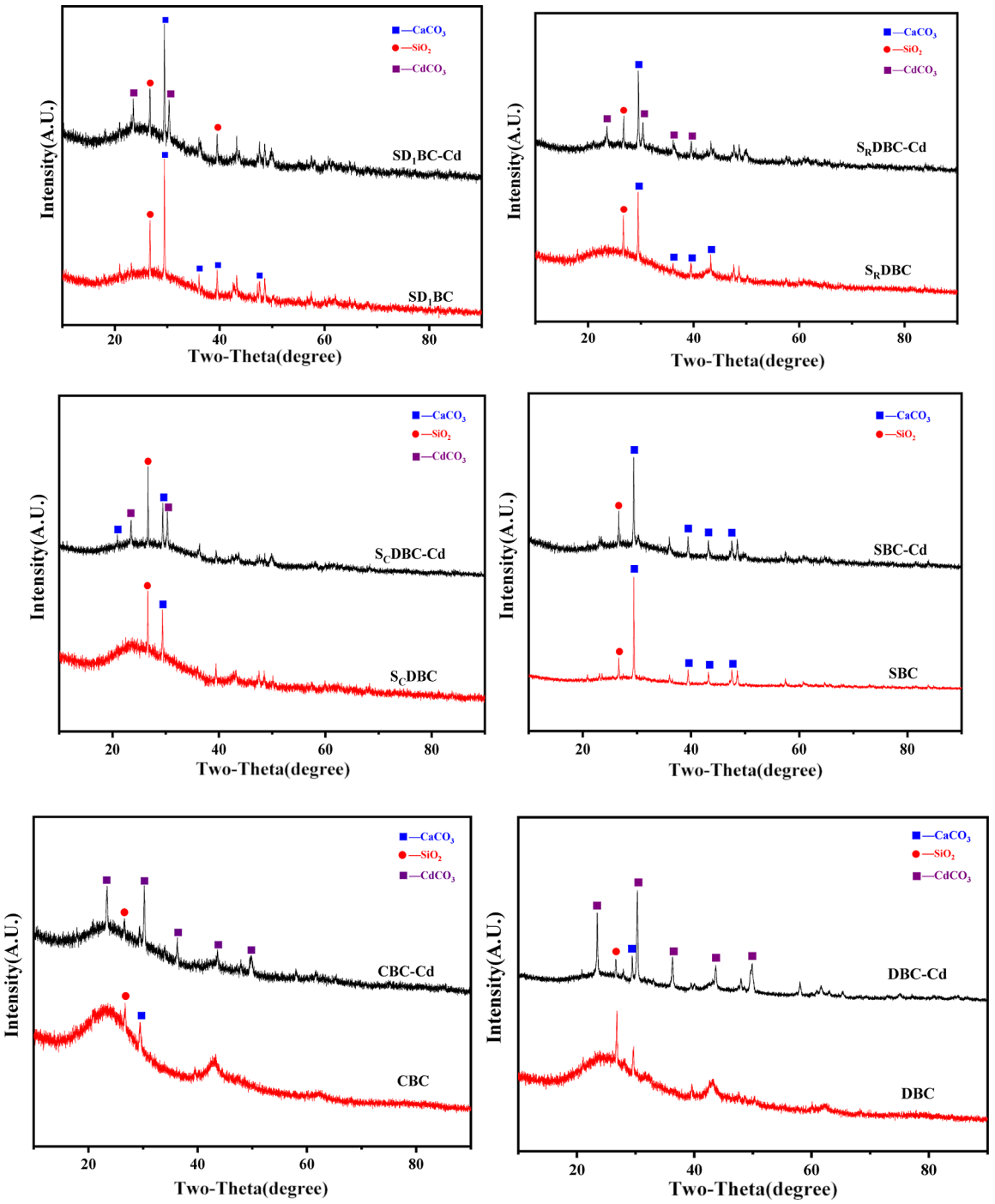

Figure 2. X-ray diffraction patterns of different biochars.

2.4. Characterization of Biochar. Fourier transform infrared spectroscopy (FTIR) (Thermo Scientific Nicolet iS5, USA) was used to identify various functional groups that existed on the surface of biochar. Scanning electron microscopy (SEM; Gemini Sigma300, Carl Zeiss AG, Germany) was used to analyze the element mapping. Ground biochar before and after Cd sorption was compared using X-ray diffraction (XRD) to discover the likely production of crystalline Cd crystals. For this analysis, a computer-controlled X-ray diffractometer (D/max 2500, Riga, Japan) with stepper motors and a graphite crystal monochromator was used. An alumina target (Al−K, hv = 1486.8 eV) was used for X-ray photoelectron spectroscopy (XPS; Thermo Scientific ESCA-LAB 250; USA) at 15 kV and 15 mA. Deconvoluted peaks were discovered using both scholarly and empirical data.

2.5. Data Analysis. For a preliminary analysis of the data, Microsoft Excel 2012 was used, and Origin 2020 was used for drawing the results. Triplicate batches of experiments were performed, including isotherms, kinetics, and the effects of pH and ion concentration.

3. RESULTS AND DISCUSSION

3.1. Characterization of Biochar. The SEM graphic of biochar under a scanning electron microscope is shown in

https://doi.org/10.1021/acsomega.3c01196
ACS Omega 2023, 8, 24912−24921

Figure 1. SBC and SD_1BC exhibited obvious agglomeration phenomena with different sizes, dense and rough surfaces, and underdeveloped pore structures. CBC revealed non-rod-like residual coke with a loose residual coke structure and more pore distribution. The SR_DBC sample had a loose surface with pores of different sizes. The surface of the SCDBC sample exhibited irregularities with unevenly distributed pores. The CBC and DBC samples were rod-shaped with a uniform pore distribution. After the carbonization of the biomass, dehydration and decarboxylation occurred, forming a highly aromatic conjugated system which retained the basic structural characteristics of biomass; the contour of each tissue was clearer, and the carbon skeleton structure was obvious.[23] Owing to the different compositions of sludge and straw combined with water and volatile organic compounds, the structures of CBC and DBC were different. Because of the higher organic matter content, sludge had a lower pyrolysis degree than straw, resulting in a significantly lower surface pore structure in sludge than straw biochar. The pore structure of biochar may be formed by the escape of volatile substances during pyrolysis, and the pore structures may have potential value in biochar performance. The rough surface of biochar may provide chemical positions, which could lead to a series of chemical reactions, such as ion exchange.

The different crystals and compositions of biochar are shown in Figure 2. In addition to organic matter, some inorganic minerals were present in the sludge, with the main mineral components being SiO_2 and $CaCO_3$. All of the biochar samples (with cadmium before and after adsorption) had two major diffraction peaks at 2θ = 26.6 and 29.5°, which aligned with conventional SiO_2 (quartz) crystallite composition and $CaCO_3$ crystals.[24] The main component of sludge was CaO, which could form $CaCO_3$ with CO_2 at high temperatures. The mineral composition was stable during pyrolysis, indicating that the biochar had compositional stability.

3.2. Cadmium(II) Adsorption. The kinetics of Cd(II) sorption by biochar are depicted in Figure 3a. The findings revealed that S_CDBC had a better Cd(II) removal capacity than other biochar preparations. Biochar required 5 h to complete most of the Cd(II) adsorption and 36 h to reach adsorption equilibrium; the adsorption rate decreased gradually with time. Previous studies reported that Cd(II) adsorption kinetics could be separated into a rapid-increase stage and a slow-equilibrium stage, with physical adsorption occurring primarily on the biochar outer surface.[25] This could be explained by the early rich vacancies on the biochar surface, which were presumably filled by prospective dangerous metal ions and grew increasingly saturated as adsorption persisted.[24]

Models of pseudo-first order (2) and pseudo-second order (3) are used to explain the sorption data. The higher square correlation coefficient ($0.836 < R^2 < 0.937$) was used in the pseudo-second order model to fit the experimental data better (Table 1). It is speculated that chemical adsorption primarily regulates the Cd(II) sorption of biochar,[26,27] including surface complexation, ion exchange, and mineral precipitation.[25,28]

Adsorption isotherms are significant in the investigation of adsorption mechanisms. The sorption performance of S_CDBC and S_RDBC was better than that of SD_1BC, SBC, CBC, and DBC, with the Cd(II) adsorption capacity as the evaluation index. As illustrated in Figure 3b, the adsorption process was revealed by analyzing the experimental data using the Freundlich and Langmuir models. Maximum Cd(II) adsorption capacity (q_m) of six biochar samples (SBC, CBC, DBC, SD_1BC, S_RDBC, and S_CDBC), estimated by the Langmuir equation, was 47.1, 24.7, 39.7, 26.3, 65.9, and 72.2 mg g^{-1}, respectively. S_CDBC demonstrated the best sorption, with a maximum adsorption capacity of 72.2 mg g^{-1}. Based on the experimental data, the fitted correlation coefficient (R^2) with the highest value (Table 2), the Langmuir model performed better than the Freundlich model in characterizing Cd(II) sorption by biochar preparations. The results demonstrated that monolayers, rather than multilayers, regulate the adsorption of Cd (II) on biochar.[29,30] Based on the fitting conditions of the adsorption model and SEM data analysis, the number of chemical binding sites was speculated to be the main factor leading to a change in adsorption performance.[25]

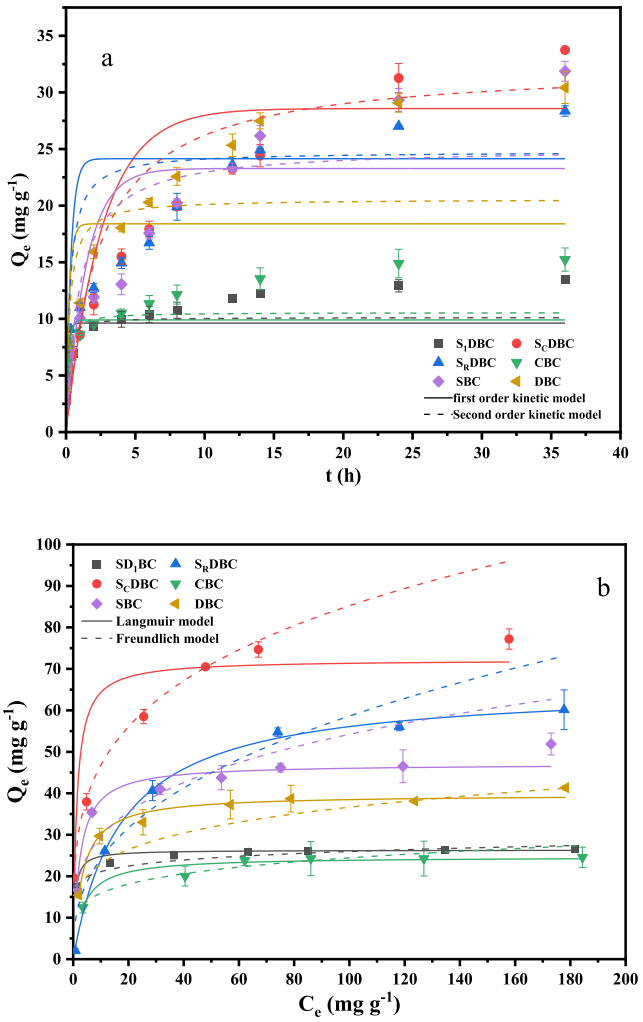

Figure 3. Kinetic adsorption (a) and isotherm of Cd (II) adsorption (b) of different biochars on Cd (II).

Table 1. Kinetic Parameters of Different Biochars Adsorbed Cd (II)

	first-order kinetic model			second-order kinetic model		
BCs	q_e	k_1	R^2	a	k_2	R^2
SD_1BC	9.62	7.42	0.869	10.1	0.948	0.912
S_RDBC	28.6	0.38	0.810	32.4	0.012	0.876
S_CDBC	24.1	2.90	0.891	24.7	0.143	0.925
CBC	9.90	5.75	0.803	10.6	0.777	0.866
SBC	23.3	0.69	0.910	25.1	0.041	0.936
DBC	18.4	4.28	0.751	20.5	0.197	0.835

https://doi.org/10.1021/acsomega.3c01196
ACS Omega 2023, 8, 24912−24921

Table 2. Isothermal Parameters of Different Biochars Adsorbed Cd (II)

	Langmuir			Freundlich		
BCs	q_m/(mg g^{-1})	K_3/(mg L^{-1})	R^2	K_4	$-\frac{1}{n}$	R^2
SD_1BC	26.31	1.60	0.99	17.14	−0.090	0.98
S_RDBC	65.87	0.057	0.99	10.04	−0.383	0.91
S_CDBC	72.22	0.813	0.98	25.66	−0.261	0.99
SBC	47.08	0.435	0.96	16.11	−0.264	0.84
CBC	24.67	0.285	0.99	10.35	−0.186	0.91
DBC	39.70	0.313	0.97	14.36	−0.203	0.97

S_CDBC was inferred to effectively increase the number of chemical binding sites, therefore, S_CDBC had better adsorption performance for Cd(II).

3.3. Influences of the Solution's Initial pH. pH influences not only the adsorbent's surface charge but also the ionization degree and morphology of metal ions in the adsorbent. Adsorption on S_CDBC at different initial pH values, and change in the solution pH before and after adsorption (Figure 4a). As the initial pH decreased from 7.0 to 5.0, the Cd(II) absorption decreased significantly from 72.2 to 43.1 mg g^{-1}. S_CDBC was illustrated to react completely with Cd(II) at higher pH values, between 5.0 and 7.0, since hydrogen ions in the solution increased with a decrease in pH and competed with Cd(II) for adsorption sites. Because there were insufficient adsorption sites left for Cd(II) to be adsorbed, the biochar adsorption capacity decreased. As the solution pH increases, the root of hydroxide combines with the hydrogen ions on the surface of the biochar, thereby reducing the electrostatic repulsion between the hydrogen ion and Cd(II). With the decrease in hydrogen ion concentration of the solution, the competition between hydrogen ions gradually weakens,[31] making it easy for Cd(II) to combine with the binding sites having negative electric charges on the biochar surface, and Cd(II) adsorption capacity increases. Under the experimental conditions, when pH was 7, the biochar Cd(II) adsorption capacity reached its maximum value. After the reaction, the pH of the solution did not significantly change, and none of them reached the pH (approximately 8.2−9.7) at which Cd(II) precipitates in the solution, demonstrating that the removal of Cd(II) was due to its adsorption on biochar rather than due to its precipitation caused by an increase in solution's pH. When the pH increased furthermore, surface complexation of the Cd(II) solution existed in the state of $Cd(OH)^+$.[32] The precipitation interaction between Cd(II) and OH^- was the main factor impacting Cd(II) removal, which reduced biochar's Cd(II) adsorption capability.[33] The increased adsorption capacity might be attributed to the dissociation of −COOH and −OH functional groups from biochar with Cd(II) and their interaction to form surface complexes.[34,35]

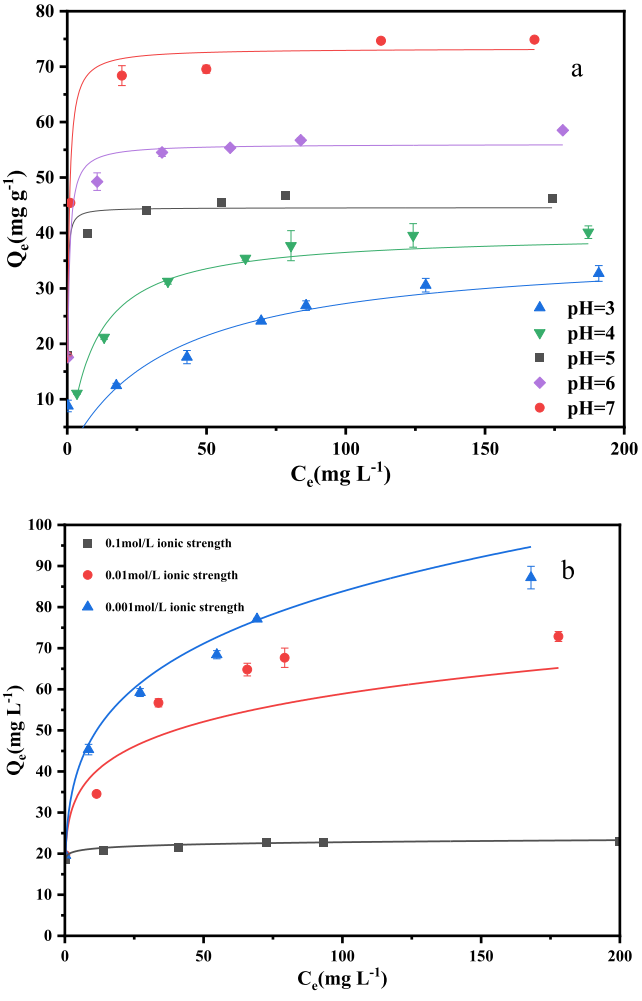

Figure 4. Effects of pH (a) and ionic strength (b) on adsorption of Cd (II) by S_cDBC.

3.4. Influences of Ionic Strength. The impact of ionic strength on the sorption of Cd(II) by S_CDBC is shown in Figure 4b. As the amount of $NaNO_3$ (0.001−0.1 mol L^{-1}) in the Cd(II) aqueous solution increased, the amount of Cd(II) that S_CDBC could adsorb decreased. The decrease in Cd(II) adsorption attributed to the rise in ionic strength may be explained by the competition between sodium ions and Cd(II) for the negatively charged adsorption sites on S_CDBC, resulting in a decrease in the biochar's adsorption performance to adsorb cadmium as the concentration of sodium nitrate increases. High ionic strength causes agglomeration of adsorbents in particle form, reducing the total number of adsorption sites and thus the adsorbed quantity.[36] Adsorption can be classified as non-specific or specific based on the influence of ionic strength on it. If the additional exogenous ions promoted adsorption, the latter occurred by internal coordination and specific adsorption; if the adsorption was inhibited, an outer complex was formed on the surface of the adsorbent, and the latter was adsorbed on the diffuse layer with opposing charges through electrostatic interactions.[37] Therefore, Cd(II) may be inferred to be adsorbed on the biochar's surface by electrostatic interactions, forming an outer−sphere complex.

https://doi.org/10.1021/acsomega.3c01196
ACS Omega 2023, 8, 24912−24921

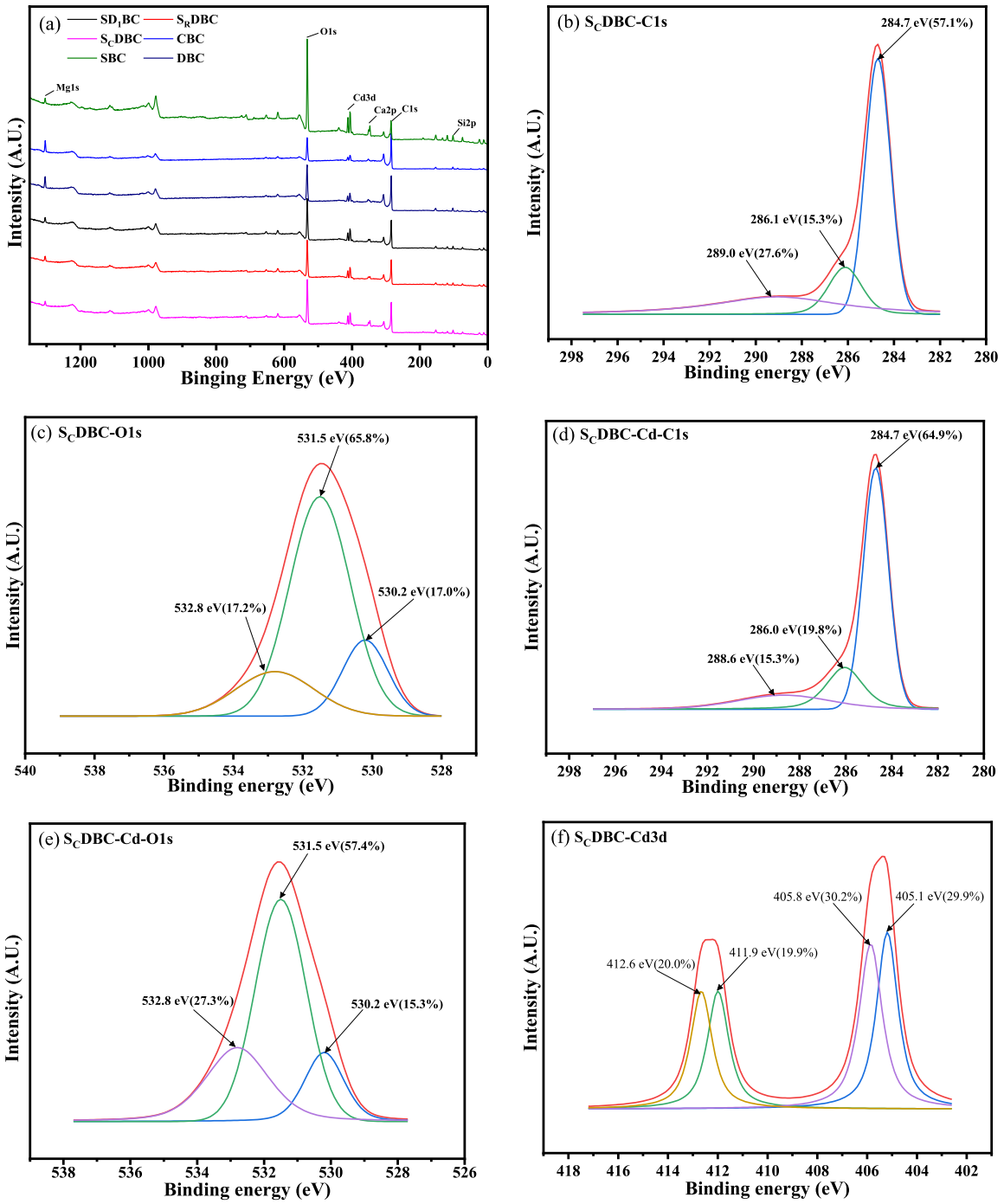

Figure 5. XPS spectrum of different biochars. (a) XPS full spectrum of biochars, (b)C 1s spectra of S_cDBC, (c) O 1s spectra of S_cDBC, (d, e, f) C 1s, O 1s, and Cd 3d spectra of S_cDBC-Cd, respectively.

3.5. Adsorption Mechanism. The FTIR spectra of the S_CDBC biochar sample and biochar-adsorbed Cd are depicted in Figure S1. The peak value of S_CDBC was approximately 3400 cm^{-1}, which was strongly connected to the stretching vibration of the interlayer of metal-OH groups or water molecules.[38] The peak value of 2880 cm^{-1} represents the tensile vibration of $-CH_2$,[39] which implied that the biochar has aromatic or aliphatic chemicals present during the process of synthesis,[40] and the weak peak was approximately 1570 cm^{-1} and showed C=C stretching vibration characteristic.[41] The peak height of 1423 cm^{-1}, which appeared in the S_CDBC after co-pyrolysis, represented the C−H bending vibration. The peak at 1030 cm^{-1} represented the stretching vibration of C−O. In addition, the peak at 878 cm^{-1} was attributable to aromatic C−H.[42] Several studies have shown that heavy metals can react with oxygen-containing functional groups; therefore, oxygen-containing functional groups could be significant in cadmium adsorption. Through comparative analysis, the functional group types of S_CDBC before and after adsorption were found to be not very different, although some absorption peaks' intensity was weakened. The −OH peak at 3400 cm^{-1} disappeared after adsorption, indicating that −OH is involved in the cadmium adsorption process. After Cd(II) sorption, the peaks of C−H (878 cm^{-1}) and C−O (1030 cm^{-1}) increased

https://doi.org/10.1021/acsomega.3c01196
ACS Omega 2023, 8, 24912−24921

slightly, demonstrating the involvement of C−H/C−O groups in adsorption and cation−π/π−π interactions between cadmium and the biochar's surface.[43,44]

Binding energy shifts for C, O, and Cd were observed using XPS to further investigate the mechanism of adsorption on S_CDBC (Figure 5a). Six types of biochar were found, all containing the absorption peaks of C, O, Cd, Mg, Ca, and Si; the primary constituents were the elements C and O, with binding energies of around 284 and 530 eV, respectively. Figure 5b illustrated the existence of three major C 1s peaks in biochar, which were attributed to the C−C/C−H, C−O, and C═O, respectively, at values of 284.7, 286.1, and 289.0 eV.[45,46] Following Cd adsorption, the biochar also showed three major C 1s peaks at 284.7, 286.0, and 288.6 eV (Figure 5d), which were ascribed to C−C, C−O−C, and O−C═O groups, respectively. The binding energy of distinct oxygen species was used to separate the O 1s XPS spectra into three overlapped peaks: M−O (530.2 eV, oxygen bonded to metal), M−OH (531.5 eV, hydroxyl linked to metal), and −C═O/C−O (532.9 eV, carbon−oxygen bond). The −OH percentage of S_CDBC before cadmium adsorption was 65.8%, which declined to 57.4% after cadmium adsorption (Figure 5c,e). This implied that the sorbent surface existed contained abundant −OH groups, which participate in cadmium sorption.[47,48] The fraction of M−O increased from 17.2 to 27.3%, as the electron-deficient metal cations decreased the electron cloud density surrounding the O atoms in −OH and −COOH to generate Cd−O.[49] In addition, Cd was detected in the adsorbents after adsorption (Figure 5f). The Cd 3d peak of Cd-loaded biochar in the XPS spectra could be observed in comparison to the XPS spectra of biochar, indicating that Cd was present on the biochar surface. Specific sorption, particularly in the form of $CdCO_3$ or Cd−O, was identified by Cd XPS analysis[50−52] and elucidated the Cd(II) removal mechanism. The peak values of the Cd 3d spectrum of S_CDBC-Cd at 405.1 and 411.9 eV were attributed to Cd 3d 5/2 and Cd 3d 3/2 respectively, indicating that Cd(II) exists as $CdCO_3$. Peak binding energies of 405.8 eV for Cd 3d 5/2 and 412.6 eV for Cd 3d 3/2, respectively, demonstrating that Cd(II) presents in the form of Cd−O.[25,53] The original summit of $CaCO_3$ was replaced by the peak of $CdCO_3$, and a new peak of $CdCO_3$ was generated from biochar with adsorbed Cd(II) in XRD. This revealed that chemical interactions may occur between the cadmium ions and $CaCO_3$ during the adsorption process, possibly combining with free CO_3^{2-} to form $CdCO_3$. The characterization of $CdCO_3$ and its formation were consistent with the earlier report.[54] Based on the discussion and analysis above, as shown in Figure 6, it was determined that surface complexation of Cd with active adsorption sites (−OH), coordination with electrons (C−H, C−O), cation−π interaction, and precipitation with inorganic anions (OH^-, CO_3^{2-}) were the possible Cd(II) adsorption mechanisms of S_CDBC.

4. CONCLUSIONS

Biochar with excellent adsorption properties was synthesized by the co-pyrolysis of sludge and corn straw to address the issues of extensive accumulation and limited utilization of sludge and straw. Compared to other sludge-based and straw-based biochar preparations, S_CDBC had the highest adsorption capacity (q_m = 72.2 mg g^{-1}). The solution pH and ionic strength affected the Cd(II) adsorption capacity of biochar. According to XPS and FTIR analysis, the main adsorption mechanism of SCDBC is primarily attributed to chemisorption. The Cd(II) adsorption of S_CDBC occurred mainly through precipitation with inorganic anions, surface complexation with active sorption sites, and coordination with π electrons. S_CDBC could be used as an effective adsorbent for mitigating Cd pollution in aquatic environments. Therefore, this study provides a novel idea for the resource utilization of municipal sludge and straw and suggests a theoretical reference for their application in the field of environmental remediation.

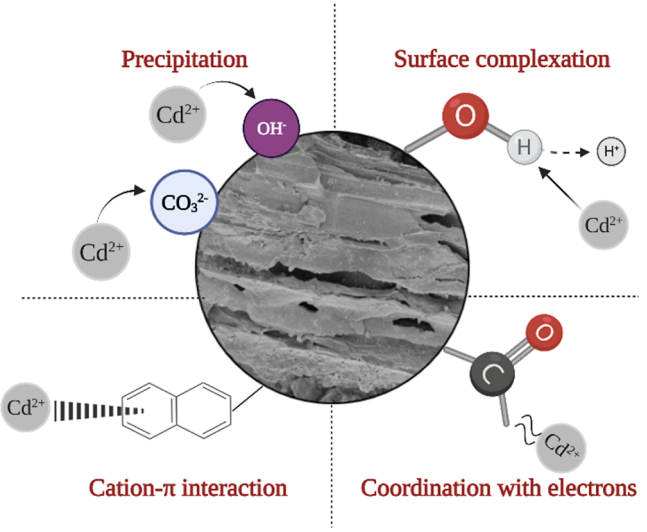

Figure 6. Adsorption mechanisms of the S_CDBC schematic diagram.

■ ASSOCIATED CONTENT

Supporting Information

The Supporting Information is available free of charge at https://pubs.acs.org/doi/10.1021/acsomega.3c01196.

Contents of main heavy metals in municipal sludge, contents of main heavy metals in different biochars, economic cost comprehensive analysis of biochar preparation, leaching contents of Cd (II) in different biochar, comparison of adsorption capacity for adsorption of Cd(II) by various adsorbents reported in the literature, and FTIR spectra of ScDBC biochar (PDF)

■ AUTHOR INFORMATION

Corresponding Authors

Minling Gao − *Department of Material and Environmental Engineering, Shantou University, Shantou 515063, China*; Email: kyforever2013@163.com

Zhengguo Song − *Guangdong Provincial Key Laboratory of Marine Disaster Prediction and Prevention, Shantou University, Shantou 515063, China*; orcid.org/0000-0003-4393-0622; Email: forestman1218@163.com

Authors

Qiaoting Chen − *Department of Material and Environmental Engineering, Shantou University, Shantou 515063, China*

Qiyu Miao − *Department of Material and Environmental Engineering, Shantou University, Shantou 515063, China*

Ling Xiao − *Department of Material and Environmental Engineering, Shantou University, Shantou 515063, China*

Zhongyang Li − *Institute of Farmland Irrigation of CAAS, Xinxiang 453002, China*

https://doi.org/10.1021/acsomega.3c01196
ACS Omega 2023, 8, 24912−24921

Weiwen Qiu − *The New Zealand Institute for Plant and Food Research Limited, Christchurch 8140, New Zealand*

Complete contact information is available at: https://pubs.acs.org/10.1021/acsomega.3c01196

Author Contributions

Q.C. and Q.M. performed laboratory experiments. L.X. and W.Q. provided significant input on the experimental design. M.G. and Z.S. conceived of the idea of this study and partly funded the study. M.G. and Z.S. analyzed the data and prepared the manuscript; all authors contributed substantially to revisions.

Notes

The authors declare no competing financial interest.

■ ACKNOWLEDGMENTS

This work was funded by the STU Scientific Research Foundation for Talents (no. NTF19026, NTF19025) and the Key Scientific and Technological Research Topics of Tibet (XZ202001ZY0048N).

■ REFERENCES

(1) Lan, J. D.; Dong, Y.; Sun, Y.; Fen, L.; Zhou, M.; Hou, H.; Du, D. A novel method for solidification/stabilization of Cd (II), Hg (II), Cu (II), and Zn (II) by activated electrolytic manganese slag. *J. Hazard. Mater.* **2021**, *409*, 124933.

(2) Liu, C.; Wu, T.; Hsu, P. C.; Xie, J.; Zhao, J.; Liu, K.; Sun, J.; Xu, J.; Tang, J.; Ye, Z.; et al. Direct/alternating current electrochemical method for removing and recovering heavy metal from water using graphene oxide electrode. *ACS Nano* **2019**, *13*, 6431−6437.

(3) Banerjee, S. S.; Chen, D. H. Fast removal of copper ions by gum arabic modified magnetic nano-adsorbent. *J. Hazard. Mater.* **2007**, *147*, 792−799.

(4) Li, S.; Li, S.; Wen, N.; Wei, D.; Zhang, Y. Highly effective removal of lead and cadmium ions from wastewater by bifunctional magnetic mesoporous silica. *Sep. Purif. Technol.* **2021**, *265*, 118341.

(5) Liu, L.; Yue, T.; Liu, R.; Lin, H.; Wang, D.; Li, B. Efficient absorptive removal of Cd(II) in aqueous solution by biochar derived from sewage sludge and calcium sulfate. *Bioresour. Technol.* **2021**, *336*, 125333.

(6) Zhang, Z.; Wang, T.; Zhang, H.; Liu, Y.; Xing, B. Adsorption of Pb(II) and Cd(II) by magnetic activated carbon and its mechanism. *Sci. Total Environ.* **2021**, *757*, 143910.

(7) Yao, Y.; Gao, B.; Chen, J.; Yang, L. Engineered Biochar Reclaiming Phosphate from Aqueous Solutions: Mechanisms and Potential Application as a Slow-Release Fertilizer. *Environ. Sci. Technol.* **2013**, *47*, 8700−8708.

(8) Joseph, S.; Peacocke, C.; Lehmann, J.; Munroe, P. Developing a Biochar Classification and Test Methods. *Biochar for environmental management: science and technology*; Taylor and Francis, 2009; Vol. *1*; pp 107−126.

(9) Higashikawa, F.; Conz, R.; Colzato, M.; Cerri, C.; Alleoni, L. Effects of feedstock type and slow pyrolysis temperature in the production of biochars on the removal of cadmium and nickel from water. *J. Cleaner Prod.* **2016**, *137*, 965−972.

(10) Yuan, H.; Lu, T.; Huang, H.; Zhao, D.; Kobayashi, N.; Chen, Y. Influence of pyrolysis temperature on physical and chemical properties of biochar made from sewage sludge. *J. Anal. Appl. Pyrolysis* **2015**, *112*, 284−289.

(11) Yuan, H.; Lu, T.; Zhao, D.; Huang, H.; Noriyuki, K.; Chen, Y. Influence of temperature on product distribution and biochar properties by municipal sludge pyrolysis. *J. Mater. Cycles Waste Manage.* **2013**, *15*, 357−361.

(12) Li, J.; Yu, G.; Xie, S.; Pan, L.; Li, C.; You, F.; Wang, Y. Immobilization of heavy metals in ceramsite produced from sewage sludge biochar. *Sci. Total Environ.* **2018**, *628-629*, 131−140.

(13) Rigby, H.; Clarke, B. O.; Pritchard, D. L.; Meehan, B.; Beshah, F.; Smith, S. R.; Porter, N. A. A critical review of nitrogen mineralization in biosolids-amended soil, the associated fertilizer value for crop production and potential for emissions to the environment. *Sci. Total Environ.* **2016**, *541*, 1310−1338.

(14) Wang, H.; Wang, F.; Sun, R.; Gao, C.; Wang, Y.; Sun, N.; Bi, Y. Policies and regulations of crop straw utilization of foreign countries and its experience and inspiration for China. *Trans. Chin. Soc. Agric. Eng.* **2016**, *32*, 216−222.

(15) Wang, H.; Xu, J.; Sheng, L. Preparation of straw biochar and application of constructed wetland in China: a review. *J. Cleaner Prod.* **2020**, *273*, 123131.

(16) Zhao, J.-N.; Zhang, G.; Yang, D. Estimation of carbon emission from burning of grain crop residues in China. *J. Agro-Environ. Sci.* **2011**, *30*, 812−816.

(17) Liu, B.; Ye, C. Preparation of biochar from co-pyrolysis of sewage sludge-corn straw and its adsorption for Pb^{2+}. *Appl. Chem. Ind.* **2018**, *47*, 1931−1935.

(18) Zhang, J.; Diao, H.; Wang, M.; Cao, Y.; Xu, S.; Zhang, j. Effects of rice husk and sewage sludge co-pyrolysis on characteristics of the sludge biochar and its ecological risk of heavy metals. *Acta Sci. Circumstantiae* **2019**, *4*, 1250−1256.

(19) Huang, S.; Luo, W.; Su, Y.; Hw, Q.; Gai, S.; Zhang, Y.; Zhou, Z. The properties of Changsha municipal sludge-rice husk mixed biochar and its application in soil. *China Tire Resour. Compr. Util.* **2020**, *38*, 34−38.

(20) Wang, Z.; Zhu, H.; Xing, W.; Song, Q.; Sun, X.; Zhang, Y. Optimization of using co-pyrolysis of sludge and straw of prepare biochar and adsorption of Cr(VI). *Environ. Eng.* **2019**, *37*, 138−142.

(21) Zhang, H.; Cao, Y.; Xu, W.; Lv, J. Decomposition characteristics of plant straw in response to changes in microbial community. *Acta Pedol. Sin.* **2019**, *56*, 1482−1492.

(22) Zama, E.; Zhu, Y.; Reid, B. J.; Sun, G. The role of biochar properties in influencing the sorption and desorption of Pb(II), Cd(II) and As(III) in aqueous solution. *J. Cleaner Prod.* **2017**, *148*, 127−136.

(23) Okimori, Y.; Ogawa, M.; Takahashi, F. Potential of CO_2 emission reductions by carbonizing biomass waste from industrial tree plantation in South Sumatra, Indonesia. *Mitig. Adapt. Strateg. Glob. Chang.* **2003**, *8*, 261−280.

(24) Feng, J.; Hu, X.; Yue, P. L. Novel Bentonite Clay-Based Fe-Nanocomposite as a Heterogeneous Catalyst for Photo-Fenton Discoloration and Mineralization of Orange II. *Environ. Sci. Technol.* **2004**, *38*, 269−275.

(25) Wu, J.; Wang, T.; Zhang, Y.; Pan, W. The distribution of Pb(II)/Cd(II) adsorption mechanisms on biochars from aqueous solution: Considering the increased oxygen functional groups by HCl treatment. *Bioresour. Technol.* **2019**, *291*, 121859.

(26) Guo, J.; Yan, C.; Luo, Z.; Fang, H.; Hu, S.; Cao, Y. Synthesis of a novel ternary HA/Fe-Mn oxides-loaded biochar composite and its application in cadmium(II) and arsenic(V) adsorption. *J. Environ. Sci.* **2019**, *85*, 168−176.

(27) Liu, P.; Rao, D.; Zou, L.; Teng, Y.; Yu, H. Capacity and potential mechanisms of Cd(II) adsorption from aqueous solution by blue algae-derived biochars. *Sci. Total Environ.* **2021**, *767*, 145447.

(28) Penido, E. S.; Melo, L. C. A.; Guilherme, L. R. G.; Bianchi, M. L. Cadmium binding mechanisms and adsorption capacity by novel phosphorus/magnesium-engineered biochars. *Sci. Total Environ.* **2019**, *671*, 1134−1143.

(29) Chen, D.; Wang, X.; Wang, X.; Feng, K.; Su, J.; Dong, J. The mechanism of cadmium sorption by sulphur-modified wheat straw biochar and its application cadmium-contaminated soil. *Sci. Total Environ.* **2020**, *714*, 136550.

(30) Syafiuddin, A.; Salmiati, S.; Jonbi, J.; Fulazzaky, M. A. Application of the kinetic and isotherm models for better understanding of the behaviors of silver nanoparticles adsorption onto different adsorbents. *J. Environ. Manage.* **2018**, *218*, 59−70.

(31) Li, L. I.; Yuchao, L. U.; Ya, L. I. U. Adsorption mechanisms of cadmium (II) on biochars derived from corn straw. *J. Agro-Environ. Sci.* **2012**, *31*, 2277−2283.
(32) Zeng, T.; Zhang, X.; Nong, H.; Hu, Q.; Wang, L.; Wang, A. Efficiency, mechanism and microbial community of Cd(II) removal by mixed bacteria enriched from heavy metals mine soil. *Trans. Nonferrous Met. Soc. China* **2022**, *32*, 3404−3419.
(33) Chen, X.; Chen, G.; Chen, L.; Chen, Y.; Lehmann, J.; McBride, M. B.; Hay, A. G. Adsorption of copper and zinc by biochars produced from pyrolysis of hardwood and corn straw in aqueous solution. *Bioresour. Technol.* **2011**, *102*, 8877−8884.
(34) Wang, Y.; Ji, H.; Lu, H.; Liu, Y.; Yang, R.; He, L.; Yang, S. Simultaneous removal of Sb(III) and Cd(II) in water by adsorption onto a $MnFe_2O_4$−biochar nanocomposite. *RSC Adv.* **2018**, *8*, 3264−3273.
(35) Khan, Z. H.; Gao, M.; Qiu, W.; Song, Z. Properties and adsorption mechanism of magnetic biochar modified with molybdenum disulfide for cadmium in aqueous solution. *Chemosphere* **2020**, *255*, 126995.
(36) Eren, E.; Afsin, B. Investigation of a basic dye adsorption from aqueous solution onto raw and pre-treated bentonite surfaces. *Dyes Pigm.* **2008**, *76*, 220−225.
(37) Mohapatra, D.; Mishra, D.; Chaudhury, G.; Das, R. Arsenic adsorption mechanism on clay minerals and its dependence on temperature. *Korean J. Chem. Eng.* **2007**, *24*, 426−430.
(38) Mitrogiannis, D.; Psychoyou, M.; Baziotis, I.; Inglezakis, V. J.; Koukouzas, N.; Tsoukalas, N.; Palles, D.; Kamitsos, E.; Oikonomou, G.; Markou, G. Removal of phosphate from aqueous solutions by adsorption onto $Ca(OH)_2$ treated natural clinoptilolite. *Chem. Eng. J.* **2017**, *320*, 510−522.
(39) Schmitt, J.; Flemming, H. C. FTIR-spectroscopy in microbial and material analysis. *Int. Biodeterior. Biodegrad.* **1998**, *41*, 1−11.
(40) Li, R.; Wang, J. J.; Zhou, B.; Zhang, Z.; Liu, S.; Lei, S.; Xiao, R. Simultaneous capture removal of phosphate, ammonium and organic substances by MgO impregnated biochar and its potential use in swine wastewater treatment. *J. Cleaner Prod.* **2017**, *147*, 96−107.
(41) Bouraada, M.; Lafjah, M.; Ouali, M. S.; Demenorval, L. Basic dye removal from aqueous solutions by dodecylsulfate-and dodecyl benzene sulfonate-intercalated hydrotalcite. *J. Hazard. Mater.* **2008**, *153*, 911−918.
(42) Cui, X.; Fang, S.; Yao, Y.; Li, T.; Ni, Q.; Yang, X.; He, Z. Potential mechanisms of cadmium removal from aqueous solution by Canna indica derived biochar. *Sci. Total Environ.* **2016**, *562*, 517−525.
(43) Zeng, Z.; Ye, S.; Wu, H.; Xiao, R.; Zeng, G.; Liang, J.; Zhang, C.; Yu, J.; Fang, Y.; Song, B. Research on the sustainable efficacy of g-MoS_2 decorated biochar nanocomposites for removing tetracycline hydrochloride from antibiotic-polluted aqueous solution. *Sci. Total Environ.* **2019**, *648*, 206−217.
(44) Kumar, S.; Masto, R. E.; Kaushik, G. Thermally processed biochar: preparation, characterisation and their application for cadmium removal from surface and groundwater. *Int. J. Environ. Anal. Chem.* **2021**, 1−20.
(45) Jing, X. R.; Wang, Y. Y.; Liu, W. J.; Wang, Y. K.; Jiang, H. Enhanced adsorption performance of tetracycline in aqueous solutions by methanol-modified biochar. *Chem. Eng. J.* **2014**, *248*, 168−174.
(46) Xu, Y.; Liu, Y.; Liu, S.; Tan, X.; Zeng, G.; Zeng, W.; Ding, Y.; Cao, W.; Zheng, B. Enhanced adsorption of methylene blue by citric acid modification of biochar derived from water hyacinth (*Eichornia crassipes*). *Environ. Sci. Pollut. Res.* **2016**, *23*, 23606−23618.
(47) Lin, J.; Zhan, Y.; Wang, H.; Chu, M.; Wang, C.; He, Y.; Wang, X. Effect of calcium ion on phosphate adsorption onto hydrous zirconium oxide. *Chem. Eng. J.* **2017**, *309*, 118−129.
(48) Lǔ, J.; Liu, H.; Liu, R.; Zhao, X.; Sun, L.; Qu, j. Adsorptive removal of phosphate by a nanostructured Fe−Al−Mn trimetal oxide adsorbent. *Powder Technol.* **2013**, *233*, 146−154.
(49) Yu, W.; Hu, J.; Yu, Y.; Ma, D.; Gong, W.; Qiu, H.; Hu, Z.; Gao, H. w. Facile preparation of sulfonated biochar for highly efficient removal of toxic Pb(II) and Cd(II) from wastewater. *Sci. Total Environ.* **2021**, *750*, 141545.
(50) Guo, Z.; Zhang, X.; Kang, Y.; Zhang, J. Biomass-derived carbon sorbents for Cd (II) removal: activation and adsorption mechanism. *ACS Sustainable Chem. Eng.* **2017**, *5*, 4103−4109.
(51) Liang, J.; Li, X.; Yu, Z.; Zeng, G.; Luo, Y.; Jiang, L.; Yang, Z.; Qian, Y.; Wu, H. Amorphous MnO_2 modified biochar derived from aerobically composted swine manure for adsorption of Pb (II) and Cd (II). *ACS Sustainable Chem. Eng.* **2017**, *5*, 5049−5058.
(52) Zhang, F.; Wang, X.; Yin, D.; Peng, B.; Tan, C.; Liu, Y.; Tan, X.; Wu, S. Efficiency and mechanisms of Cd removal from aqueous solution by biochar derived from water hyacinth (*Eichornia crassipes*). *J. Environ. Manage.* **2015**, *153*, 68−73.
(53) Yin, G.; Song, X.; Tao, L.; Sarkar, B.; Sarmah, A. K.; Zhang, W.; Lin, Q.; Xiao, R.; Liu, Q.; Wang, H. Novel Fe-Mn binary oxide-biochar as an adsorbent for removing Cd(II) from aqueous solutions. *Chem. Eng. J.* **2020**, *389*, 124465.
(54) Shan, R.; Yan, L.; Yang, K.; Hao, Y.; Du, B. Adsorption of Cd (II) by Mg−Al−CO_3-and magnetic Fe_3O_4/Mg−Al−CO_3-layered double hydroxides: Kinetic, isothermal, thermodynamic and mechanistic studies. *J. Hazard. Mater.* **2015**, *299*, 42−49.

https://doi.org/10.1021/acsomega.3c01196
ACS Omega 2023, 8, 24912−24921